

On the Oxidation of Iron in $\text{CO}_2 + \text{CO}$ Mixtures. III: Coupled Linear Parabolic Kinetics

Rune Bredesen*† and Per Kofstad*

Received June 18, 1990; revised November 14, 1990

High-purity iron has been oxidized at 1000–1200°C in CO_2 and in $\text{CO}_2 + \text{CO}$ with different compositions and at different total gas pressures (0.1–1 atm.). The experimental work has comprised thermogravimetric reaction rate measurements and characterization of the wüstite scales by metallography and x-ray diffraction. The overall results have been analyzed in terms of a classical model for coupled linear/parabolic kinetics, where it is assumed that the surface of growing wüstite scales has exactly the same defect structure and defect concentrations as that of bulk wüstite equilibrated in the same gaseous atmospheres. Important discrepancies are found between the predicted and the experimentally observed reaction behavior. Thus, both the linear and parabolic rate constants are found to be dependent on the partial pressure of CO_2 and the total gas pressure of the $\text{CO}_2 + \text{CO}$ gas mixtures, and furthermore, the reaction in $\text{CO}_2 + \text{CO}$ is slower than in O_2 and in $\text{H}_2\text{O} + \text{H}_2$ with the same oxygen activity. In order to explain the experimental results, it is suggested that CO and CO_2 molecules interact with the wüstite surface and thereby affect the defect structure and defect concentrations in a thin surface layer, and that this, in turn, affects both the linear and parabolic reaction rates.

KEY WORDS: iron; oxidation in $\text{CO}_2 + \text{CO}$ mixtures; coupled linear/parabolic kinetics; reaction mechanisms.

INTRODUCTION

High temperature oxidation of iron in CO_2 and $\text{CO}_2 + \text{CO}$ mixtures may in gross terms be considered to involve a surface reaction resulting in formation

*Department of Chemistry, University of Oslo, P.O. Box 1033 Blindern, 0315 Oslo 3, Norway.

†Permanent address: Senter for Industriforskning, P.O. Box 124 Blindern, 0314 Oslo 3, Norway.

of oxide and outward diffusional transport of iron through the scale.¹⁻⁹ Accordingly, the reaction kinetics have been interpreted in terms of coupled linear/parabolic kinetics.^{2,4-6,10}

However, detailed examinations of the reaction behavior show that additional phenomena are superimposed on ideal linear/parabolic reaction behavior.¹⁰ This is reflected in the kinetics of the reaction which may in general be described by S-shaped curves. The initial oxidation comprises formation of a film or thin scale of wüstite, and during this stage of the oxidation the texture and orientation of the oxide on each metal grain is directly related to that of the metal grains. The growth of this first film may, depending on the reaction conditions, approach linear kinetics. However, as the scale grows, the reaction rate gradually increases and this behavior is associated with a gradual change in the overall texture and morphology of the scale to a preferred orientation, where the {001} planes of the entire wüstite scale are parallel to the iron surface. It is concluded that this increased rate reflects that the preferred {001} texture provides a larger number of reaction sites in the wüstite scale surface. With further scale growth, the reaction rate goes through a maximum and then decreases with time, as iron diffusion through the scale becomes increasingly important as a rate-limiting factor.

A model for coupled kinetics combining a surface reaction and diffusional transport through the scale has been advanced by C. Wagner,¹² and this model has been used by Pettit and B. Wagner⁴ in interpreting experimentally measured reaction rates of the oxidation of iron in $\text{CO}_2 + \text{CO}$ mixtures at high temperatures. The theoretical model seemingly provides a good description of the experimental results. However, as will be shown later in this paper, Pettit and Wagner did not follow the oxidation for sufficiently long time periods to ascertain the detailed applicability of the theoretical treatment.

This work is part of an extended investigation of oxidation of iron in CO_2 and $\text{CO}_2 + \text{CO}$ mixtures. The studies which cover the initial oxidation involving growth of films and thin scales of wüstite have been described elsewhere.^{9,10} This paper focuses on long-term, parabolic-like oxidation and growth of wüstite scales with thicknesses up to several hundred microns with the purpose of delineating and studying in more detail the coupled linear/parabolic growth of wüstite scales in $\text{CO}_2 + \text{CO}$ mixtures. As Wagner's classical treatment of coupled linear/parabolic kinetics is generally accepted to be applicable, it is appropriate to review the model and its implications.

Classical Model for Coupled Linear/Parabolic Kinetics

In the classical treatment of linear/parabolic kinetics, an important basic assumption is that the composition, the defects, and defect structure

of the surface of wüstite scales growing in CO₂ + CO mixtures are exactly the same as that of bulk wüstite equilibrated in the same atmospheres. This implies that there are no "surface effects" (i.e., the surface energy does not affect the composition and defect structure of the wüstite surface to any significant extent), and there are no enrichments in the surface of the components in the gas. Furthermore, and as regards wüstite, no account has been taken of the possible presence of defect clusters in growing wüstite scales, and the chemical diffusion coefficient in wüstite, \tilde{D} , is generally assumed to be independent of the nonstoichiometry in wüstite. The nonstoichiometry, defects, and transport properties are assumed to be the same in wüstite equilibrated for extended periods at high temperatures as in growing wüstite scales.

On this basis, the outward flux of iron through the growing wüstite layer, j_{Fe} , may be written

$$j_{\text{Fe}} = \frac{M_O \tilde{D} \delta'}{V^2 \frac{\Delta m}{A}} \left(\frac{\delta^*}{\delta'} - 1 \right) \quad (1)$$

where M_O is the atomic weight of oxygen, V the molar volume of wüstite, δ' the iron deficit at the iron/wüstite interface, and δ^* the instantaneous iron deficiency at the scale/gas interface at a weight gain per surface area of $\Delta m/A$. It is implied in the model that the iron deficit at the wüstite/gas interface, δ^* , gradually increases as oxidation proceeds during the coupled kinetics.

The flux of iron is related to the net rate of incorporation of oxygen into the wüstite lattice, j_O , by

$$j_{\text{Fe}} = (1 - \bar{\delta}) j_O \quad (2)$$

where $\bar{\delta}$ is the average metal deficit in the scale.

In a previous paper dealing with initial oxidation of iron, different models for the surface reaction mechanism have been analyzed,¹⁰ and in general the expression for j_O may be written

$$j_O = \mathcal{K} f(a_{\bar{O}}^*) \left(1 - \frac{a_{\bar{O}}^*}{a_O} \right) p_{\text{CO}_2} \quad (3)$$

where $a_{\bar{O}}^*$ is the instantaneous oxygen activity in the wüstite surface (defined as $a_{\bar{O}}^* = p_{\text{CO}_2}^*/p_{\text{CO}}^*$, where $p_{\text{CO}_2}^*$ and p_{CO}^* are the partial pressures of CO₂ and CO that corresponds to $a_{\bar{O}}^*$), and a_O is the oxygen activity of the ambient gas ($a_O = p_{\text{CO}_2}/p_{\text{CO}}$, where p_{CO_2} and p_{CO} are the partial pressures of CO₂ and CO in the ambient gas mixture). The rate of dissociation of CO₂ is assumed to be rate-determining for the surface reaction, and \mathcal{K} is the rate constant

for the surface reaction, and its value depends on the number of adsorption/reaction sites on the surface. The function $f(a_{\delta}^*)$ depends on the exact nature of the mechanism of the surface reaction and the assumed defect structure of wüstite.

The rate of weight gain (uptake of oxygen) is given by

$$\frac{d}{dt} \frac{\Delta m}{A} = M_o j_o = \frac{M_o}{(1-\bar{\delta})} j_{re} \quad (4)$$

In further treatment of this expression it is convenient to introduce the following variables:

$$\frac{\Delta m}{A} = \frac{\Delta m^*}{A} \xi \quad (5)$$

$$t = t^* \nu \quad (6)$$

where

$$\frac{\Delta m^*}{A} = \frac{M_o \tilde{D} \delta'}{\mathcal{K} p_{CO_2} V^2 (1-\bar{\delta})} \quad (7)$$

and

$$t^* = \frac{\tilde{D} \delta'}{(\mathcal{K} p_{CO_2} V)^2 (1-\bar{\delta})} \quad (8)$$

If \tilde{D} and \mathcal{K} are constants and independent of a_{δ}^* (i.e., the nonstoichiometry and defect structure in the surface) and time, then $\Delta m^*/A$ and t^* are also constants, and the reaction kinetics are given by the variations in ξ and ν . By comparing Eqs. (2) and (5), it is seen ξ is given by

$$\xi = \frac{\left(\frac{\delta^*}{\delta'} - 1\right)}{f(a_{\delta}^*) \left(1 - \frac{a_{\delta}^*}{a_o}\right)} = \frac{A(a_{\delta}^*)}{B(a_{\delta}^*)} \quad (9)$$

In order to further evaluate Eq. (9), it is necessary to relate a_{δ}^* and δ^* . Such relations have in a number of investigations been determined for wüstite equilibrated in $CO_2 + CO$ mixtures.¹³⁻¹⁷ According to Giddings and

Gordons,¹⁸ who have analyzed these studies, the relations at 1000 and 1200°C may be expressed by

$$\log a_{\delta}^* = \frac{11.664}{1 - \delta^*} - 12.626 \quad (1000^{\circ}\text{C}) \quad (10)$$

$$\log a_{\delta}^* = \frac{12.078}{1 - \delta^*} - 13.170 \quad (1200^{\circ}\text{C}) \quad (11)$$

Furthermore, a relation between ξ and v may be obtained by differentiating and combining Eqs. (5) and (6) and comparing the result with Eq. (4). This leads to the expressions

$$\frac{d\xi}{dv} = \frac{\left(\frac{\delta^*}{\delta'} - 1\right)}{\xi} = \frac{A(\xi)}{\xi} \quad (12)$$

or

$$\frac{d\xi}{dv} = f(a_{\delta}^*) \left(1 - \frac{a_{\delta}^*}{a_o}\right) = B(\xi) \quad (13)$$

where A and B are expressed as functions of ξ .

In order to use this model to predict the weight gain as a function of time, it is necessary to know the values of \mathcal{K} and $\tilde{D}\delta'$. If the reaction follows ideal linear/parabolic kinetics, and thus that the linear surface reaction predominates during the initial reaction, the value of \mathcal{K} may be determined from the initial reaction rate provided $f(a_{\delta}^*)$ is known [see Eqs. (3) and (4)]. However, this approach may not be used for oxidation of iron as the reaction rate for the initial scale formation gradually increases due to a change in the texture and orientation of the scale under these conditions.

Previously, it has been assumed that the maximum rates—which are only approximately linear over a limited time period—represent the real linear rates of oxidation, and that $\delta^* \approx \delta'$ during this time period. This assumption implies that the scales are completely reoriented during conditions of maximum rates, and furthermore, as shown in Ref. (10), this also implies that the value of \tilde{D} is much higher than reported from measurements on equilibrated wüstite.

In order to obtain values of $\tilde{D}\delta'$, Eq. (4) may be arranged and combined with Eq. (1). This yields the relation

$$\tilde{D}\delta' = \frac{(1-\bar{\delta})V^2}{M_O^2\left(\frac{\delta^*}{\delta'}-1\right)} \frac{\Delta m}{A} \frac{d\frac{\Delta m}{A}}{dt} \quad (14a)$$

If \tilde{D} may be assumed to be independent of δ^* , the values $\tilde{D}\delta'$ can be estimated from the parabolic rate constants in oxygen, k_{p,O_2} , in $2(\Delta m/A)d(\Delta m/A) = k_{p,O_2} dt$, and by setting $\delta^* = \delta''$, where δ'' is the iron deficit in wüstite in equilibrium with magnetite. $\tilde{D}\delta'$ may then be written

$$\tilde{D}\delta' = \frac{(1-\bar{\delta})V^2}{2M_O^2\left(\frac{\delta''}{\delta'}-1\right)} k_{p,O_2} \quad (14b)$$

By combining Eqs. (7) and (14b), $\Delta m^*/A$ may be written

$$\frac{\Delta m^*}{A} = \frac{k_{p,O_2}}{2M_O \mathcal{K} p_{CO_2} \left(\frac{\delta''}{\delta'}-1\right)} \quad (15)$$

Furthermore, by combining Eqs. (8) and (14b), t^* is given by

$$t^* = \frac{k_{p,O_2}}{2(M_O \mathcal{K} p_{CO_2})^2 \left(\frac{\delta''}{\delta'}-1\right)} \quad (16)$$

Finally, it is seen that the relation between $\Delta m^*/A$ and t^* becomes

$$\frac{\Delta m^*}{A} \frac{1}{t^*} = M_O \mathcal{K} p_{CO_2} \quad (17)$$

From these relations it is seen that if k_{p,O_2} , \mathcal{K} , and $f(a_{\delta}^*)$ are known, it is possible to calculate the rates of the reaction during coupled linear/parabolic kinetics.

Previous investigators have used different expressions for the surface reaction. Thus, Morris and Smeltzer⁶ assumed that $f(a_{\delta}^*) = 1$, while Pettit and Wagner⁴ and Grabke¹⁹ used $f(a_{\delta}^*) = a_{\delta}^{*-2/3}$ based on isotopic exchange measurements on wüstite specimens equilibrated in $CO_2 + CO$ mixtures. (It may be noted that the value of $n = 2/3$ in a_{δ}^{*-n} is interpreted to reflect that the iron vacancy equilibrium ($\frac{1}{2}O_2 = O_O + V_{Fe}'' + 2h$) predominates in the

wüstite surface). In the following the model will be used to calculate reaction rates using different values of n in $f(a_0^*) = a_0^{*-n}$ and to compare these with experimentally measured values.

MATERIALS AND METHODS

Oxidation rates of high purity iron (99.99+) were measured by thermogravimetry. The iron specimens were cut from plates with thicknesses ranging from 1–2 mm. The total surface areas of the specimens were 2–8 cm². Further details of the specimen preparation and the experimental methods have been described elsewhere.⁹

X-Ray Diffraction

The x-ray diffraction measurements on quenched specimens were carried out on a x-ray diffractometer with crystal monochromatized Cu K_{α} radiation. The monochromator was placed between the specimen and the counter to avoid fluorescent radiation from iron in the sample to be recorded. Due to high absorption of the x-rays, a surface layer of thickness 1 μm gives rise to about 50% of the diffracted intensity, and a layer of 3 μm to 90% of the recorded scattering. All the diffractograms gave sharp crystalline reflections, and there was no sign of an amorphous background.

Quenching of the specimens was performed by dropping the specimens about 45 cm from the hot zone of the furnace onto a brass cup that was immersed in a solution of acetone and solid CO₂.

RESULTS AND DISCUSSION

Thermogravimetric Rate Measurements

Thermogravimetric studies of oxidation of iron were carried out at 1000–1200°C in CO₂ and CO₂ + CO mixtures with different compositions and at different total gas pressures. Figures 1 and 2 show results of the measurements and, as may be seen, the rates and detailed kinetics depend both on the composition and total pressure of the gas mixtures.

A primary aim of this work is to delineate and study the parabolic reaction behavior. As the oxidation involves coupled kinetics, it is important that the data are treated and plotted so as to obtain as correct values as possible of the parabolic rate constants under different experimental conditions. In this respect, three different approaches have been used.

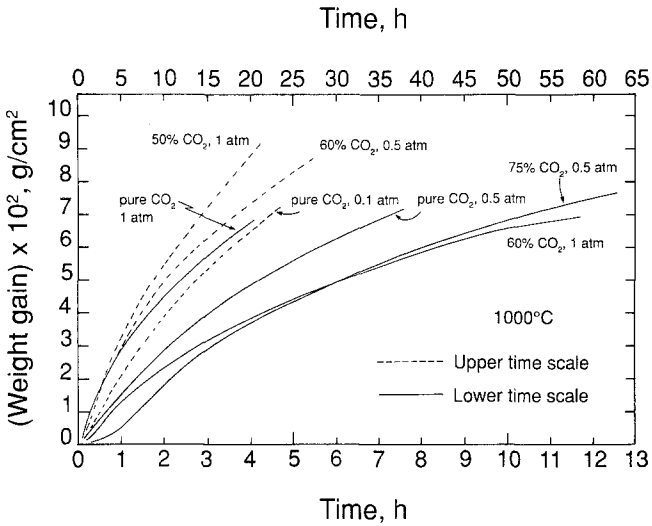


Fig. 1. The weight gain as a function of time for the oxidation of iron at 1000°C in various CO₂+CO gas mixtures with different total gas pressures.

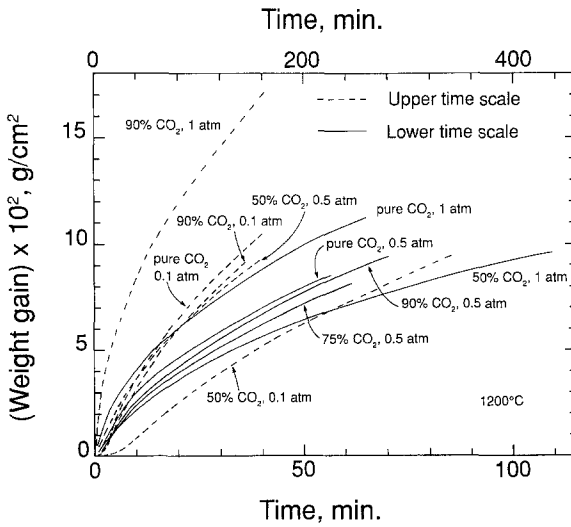


Fig. 2. The weight gain as a function of time for the oxidation of iron at 1200°C in various CO₂+CO gas mixtures with different total gas pressures.

As the integrated form of the parabolic rate equation is given by

$$\left(\frac{\Delta m}{A}\right)^2 = k_p t + C \quad (18)$$

where k_p is the parabolic rate constant and C the integration constant, it is common to evaluate k_p from plots of $(\Delta m/A)^2$ vs. t . Accordingly, values of k_p were evaluated from this type of plot.

However, for reactions which involve a significant initial nonparabolic stage, this type of plot may give inaccurate values of k_p unless the reaction is followed for a long period of time. As shown by Pieraggi²⁰ plots of $\Delta m/A$ vs. $t^{1/2}$ are preferable and give more accurate values of k_p . This latter procedure was therefore also used, and in all cases this type of plot gave higher values of k_p than those from the $(\Delta m/A)^2$ vs. t plots.

As a third alternative, the results were also plotted according to the general linear/parabolic equation, which has the form²¹

$$\left(\frac{\Delta m}{A}\right)^2 + B \frac{\Delta m}{A} = k_p(t + \tau) \quad (19a)$$

or

$$\frac{\Delta m}{A} + B = k_p \frac{(t + \tau)}{\frac{\Delta m}{A}} \quad (19b)$$

where τ is a time coordinate which corrects for the presence of an oxide layer prior to the linear oxidation. The ratio k_p/B equals the linear rate constant (i.e., $k_{\text{lin}} = k_p/B$).

Following Eq. (19b), the rate measurements may be analyzed by plotting $\Delta m/A$ vs. $t/\Delta m/A$, and for extended exposures (where $t \gg \tau$) the parabolic rate constant is given by the slope of the straight-line relationship. The values of k_{lin} may further be evaluated from the intercept obtained by extrapolating the straight lines at extended reaction to $\Delta m/A = 0$.

Figure 3 shows examples of plots by Eq. (19b). In all cases there is deviation from straight-line relationship at the smaller values of $\Delta m/A$. This deviation is due to the period with increasing rate of reaction during the initial oxidation (see for instance Refs. 9 and 10).

The values of k_p obtained from the $\Delta m/A$ vs. $t^{1/2}$ plots and from Eq. (19b) (linear/parabolic equation) were in all cases in good agreement. These values of k_p are used in the following analysis of the results.

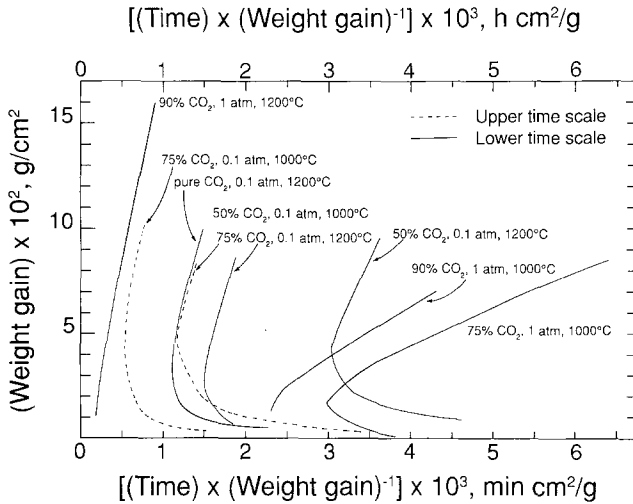


Fig. 3. The weight gain as a function of (time/weight gain) for the oxidation of iron at 1000 and 1200°C in various CO₂ + CO gas mixtures with different total gas pressures.

Linear Oxidation Rate Constants

The linear oxidation rate constants under different experimental conditions were evaluated from the plots of the linear/parabolic equation [Eq. (19b)] and the values are listed in Table I. The gas pressure dependence of the rate constant provides important clues as to the reaction mechanism of the linear reaction—and, interestingly, the results suggest that k_{lin} is dependent not only on the partial pressure of CO₂, but also on the total gas pressure of the CO₂ + CO mixtures. Both at 1000 and 1200°C, the best description of the gas pressure dependence appears to be

$$k_{lin} = k_{lin}^0 N_{CO_2} p_{CO_2} + C \quad (20)$$

where N_{CO_2} is the mole fraction of CO₂ in the gas mixture, and k_{lin}^0 and C are constants. This is illustrated in Fig. 4. It may be noted that the straight lines go through the origin of the coordinate axes, and thus the constant C in Eq. (20) is small or close to zero. Possible mechanism of the linear reaction will be discussed below.

Parabolic Rate Constants

The experimental values k_p are listed in Table I (column 5). The classical model predicts that the parabolic rate constant is only a function of the

Table I.

Gas mixture (%CO ₂ + %CO)	P_{tot} (atm)	Temp. (°C)	K_{lin} (g/cm ² sec)	K_p (g ² /cm ⁴ sec)
pure CO ₂	1	1000	2.1×10^{-5}	4.0×10^{-7}
95 + 5	1	1000	1.6×10^{-5}	4.1×10^{-7}
90 + 10	1	1000	1.3×10^{-5}	3.9×10^{-7}
75 + 25	1	1000	1.0×10^{-5}	3.0×10^{-7}
60 + 40	1	1000	6.9×10^{-6}	1.7×10^{-7}
50 + 50	1	1000	2.9×10^{-6}	1.8×10^{-7}
pure CO ₂	0.5	1000	8.8×10^{-6}	2.9×10^{-7}
95 + 5	0.5	1000	7.8×10^{-6}	2.9×10^{-7}
75 + 25	0.5	1000	5.3×10^{-6}	2.0×10^{-7}
60 + 40	0.5	1000	2.8×10^{-6}	1.3×10^{-7}
50 + 50	0.5	1000	1.9×10^{-6}	1.1×10^{-7}
pure CO ₂	0.1	1000	2.1×10^{-6}	1.0×10^{-7}
75 + 25	0.1	1000	1.4×10^{-6}	5.0×10^{-8}
50 + 50	0.1	1000	3.4×10^{-7}	3.8×10^{-8}
pure CO ₂	1	1200	2.6×10^{-4}	3.7×10^{-6}
95 + 5	1	1200	2.3×10^{-4}	3.1×10^{-6}
90 + 10	1	1200	2.1×10^{-4}	3.1×10^{-6}
75 + 25	1	1200	1.6×10^{-4}	2.7×10^{-6}
50 + 50	1	1200	8.1×10^{-5}	1.8×10^{-6}
pure CO ₂	0.5	1200	1.2×10^{-4}	2.7×10^{-6}
90 + 10	0.5	1200	8.3×10^{-5}	2.9×10^{-6}
75 + 25	0.5	1200	6.2×10^{-5}	2.7×10^{-6}
50 + 50	0.5	1200	2.4×10^{-5}	1.5×10^{-6}
pure CO ₂	0.1	1200	2.2×10^{-5}	2.2×10^{-6}
90 + 10	0.1	1200	1.9×10^{-5}	2.1×10^{-6}
75 + 25	0.1	1200	1.4×10^{-5}	2.1×10^{-6}
50 + 50	0.1	1200	6.7×10^{-6}	1.4×10^{-6}

oxygen activity of the ambient gas under conditions where only wüstite is formed, while it should be independent of the oxygen activity under conditions where bulk thermodynamic properties of the iron oxides predicts that magnetite should be formed as a thin outer layer. However, the experimental values of the parabolic rate constant clearly suggests a more complicated gas pressure dependence. This also illustrated in Fig. 5, where the values of k_p at 1000 and 1200°C are plotted as a function of $p_{\text{CO}_2}/p_{\text{CO}}$ (i.e., as a function of the oxygen activity of the ambient gas mixtures). The values of k_p in oxygen gas and in H₂O + H₂ (Refs. 22, 23) are also included in the figures. A noteworthy feature is that the rate constants in CO₂ and CO₂ + CO are lower than those in oxygen and in H₂O + H₂ and also decrease with the total pressure of the gas mixtures.

It is difficult from the available results to give an unequivocal expression for the dependence of k_p on the gas composition and the total gas pressure

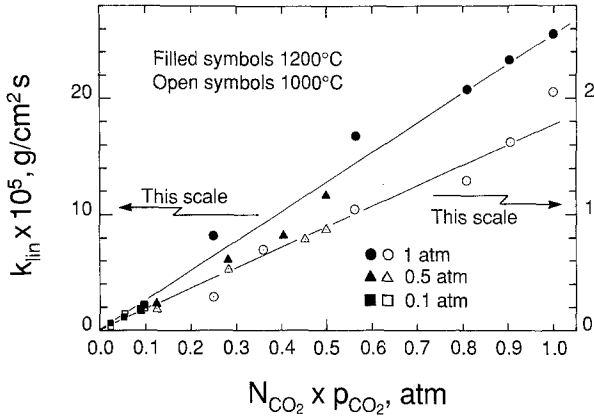


Fig. 4. The value of the surface rate constant, k_{fm} , of the oxidation of iron at 1000 (right-hand scale) and 1200°C (left-hand scale) in different $\text{CO}_2 + \text{CO}$ mixtures and total gas pressures as a function of the mole ratio of CO_2 , N_{CO_2} , multiplied by the partial pressure of CO_2 , p_{CO_2} .

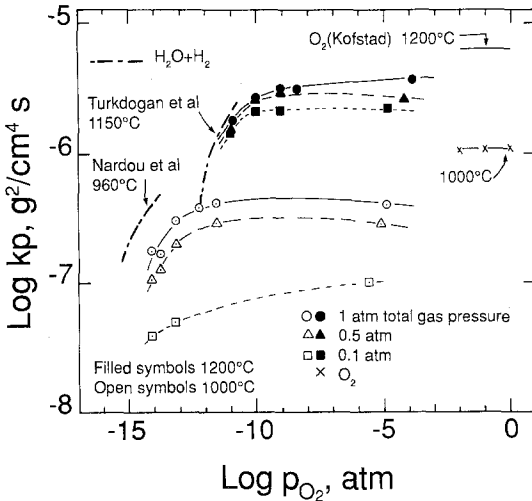


Fig. 5. The value of the parabolic rate constant, k_p , of the oxidation of iron at 1000 and 1200°C in oxygen and in different $\text{CO}_2 + \text{CO}$ mixtures with different total gas pressures as a function of the ratio of the partial pressure of CO_2 and the partial pressure of CO , $p_{\text{CO}_2}/p_{\text{CO}}$. The graph also includes previously reported results by Nardou *et al.*²³ and Turkdogan *et al.*²² in $\text{H}_2\text{O} + \text{H}_2$ mixtures.

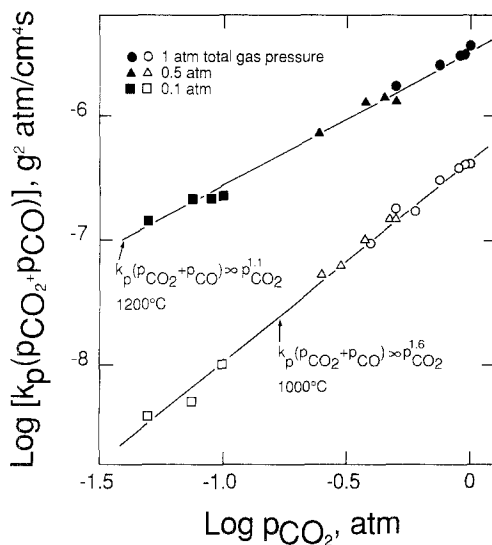


Fig. 6. The value of the parabolic rate constant multiplied by the total gas pressure, $k_p(p_{\text{CO}_2} + p_{\text{CO}})$, of the oxidation of iron at 1000 and 1200°C as a function of the partial pressure of CO₂, p_{CO_2} .

of the gas mixtures. But from the plots in Fig. 6, the following relations are suggested:

$$k_p = N_{\text{CO}_2} p_{\text{CO}_2}^{2/3} \quad 1000^\circ\text{C} \quad (21)$$

$$k_p = N_{\text{CO}_2} p_{\text{CO}_2}^{0.1} \quad 1200^\circ\text{C} \quad (22)$$

All in all, the results suggest that the classical model does not give a satisfactory description of the reaction behavior. But before making a final conclusion, let us also compare the kinetics calculated by the classical model with the observed kinetics.

Comparison of Predicted and Observed Kinetics

In order to calculate the weight gain as a function of time from the classical model, values of \mathcal{K} and \bar{D} must be known or evaluated. However, in a previous paper on the initial oxidation of iron it has been shown that \mathcal{K} and \bar{D} are interrelated and that separate values of \mathcal{K} and \bar{D} cannot be evaluated from studies of the oxidation kinetics. Thus, in order to make calculations of the weight gain, values must either be assigned to \mathcal{K} or \bar{D} . It appears most appropriate to assign a value to \bar{D} , as the chemical diffusion

coefficient has been studied independently by several investigators and is known at least within an order of magnitude.²⁴⁻²⁷

An expression for \mathcal{K} is obtained by combining and rearranging Eqs. (1), (3), and (4), and is given by

$$\mathcal{K} = \frac{M_o \tilde{D} (\delta^* - \delta')}{V^2 (1 - \bar{\delta}) \frac{\Delta m}{A} p_{\text{CO}_2} f(a_o^*) \left(1 - \frac{a_o^*}{a_o}\right)} \quad (23)$$

Furthermore, the relation between the deviation from stoichiometry in the wüstite surface, δ^* , is through combination of Eqs. (1) and (4) given by

$$\delta^* = \frac{d \frac{\Delta m}{A} (1 - \bar{\delta}) V^2 \frac{\Delta m}{A}}{dt \frac{M_o^2 \tilde{D}}{A}} + \delta' \quad (24)$$

These relations have been used to estimate values of \mathcal{K} for different values of $f(a_o^*)$ [i.e., for values of n (in a_o^{*-n}) = 0, 1, 2, and 3], by using the values of $d(\Delta m/A)/dt$ ($=k_{\text{max}}$, see Ref. 10) and $\Delta m/A$ (see Ref. 9) at the maximum rates of reaction. The corresponding values of $\Delta m^*/A$ and t^* may then be calculated for different values of n ; and from these one may, in turn, calculate the weight gain vs. time for oxidation under different experimental conditions.

Examples of comparisons between calculated and measured values under different experimental conditions are shown in Figs. 7 and 8. Table II

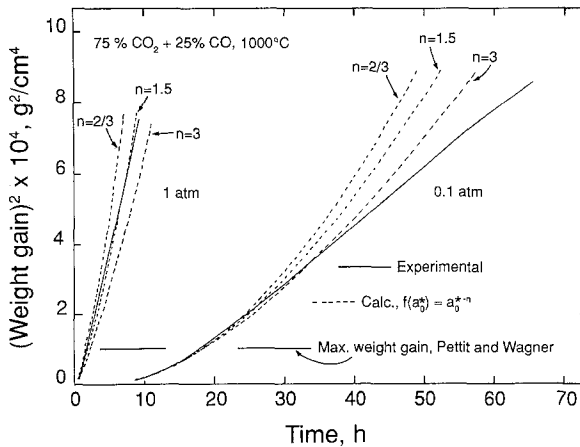


Fig. 7. Calculated and experimental curves of weight gain vs. time of the oxidation of iron at 1000°C in 75%CO₂ + 25%CO at 1 and 0.1 atm. total gas pressure.

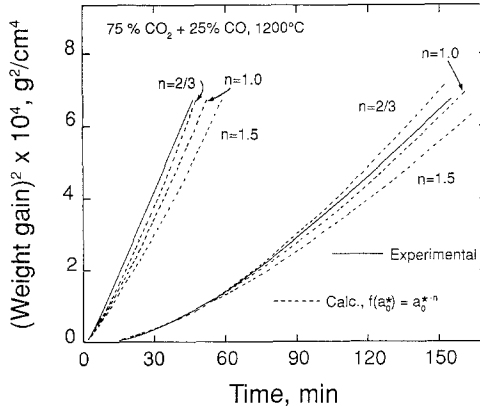


Fig. 8. Calculated and experimental curves of weight gain vs. time of the oxidation of iron at 1200°C in 75%CO₂+25%CO at 1 and 0.1 atm. total gas pressure.

shows the values of k_{max} and weight gain at the maximum rate of reaction which have been used to calculate the curves in Figs. 7 and 8. If the experimental values of k_p shown in Fig. 5 are used to calculate $\Delta m^*/A$ and t^* , from Eqs. (15) and (16), instead of the values of \tilde{D} indicated in Table II, the calculated curves increase faster than the experimentally determined curves for $n < 1$ at all experimental conditions.

It may be noted that as the initial reaction rates increase with time, zero time for the reactions have been estimated by linearly extrapolating the maximum rates of the reaction to zero weight gain.

Some important aspects are evident from these comparisons between calculated and measured reaction rates:

1. During the initial oxidation, there are only small differences in the calculated weight gains for the different models (different values of n). This is because the change in a_g^* is small during the initial oxidation so that the values of n is of less importance for the reaction

Table II.

% (CO ₂)	P_{tot} (atm)	Temp. (°C)	$k_{max} \cdot 10^6$ (g/cm ² sec)	$\Delta m/A$ (mg/cm ²)	$\tilde{D} \cdot 10^6$ (cm ² /sec)	V (cm ³ /mol)	δ'
75	1	1000	6.5	5.0	3.0	12.54	0.0457
75	0.1	1000	0.64	14.5	3.0	12.54	0.0457
75	1	1200	87.9	4.0	15.0	12.66	0.0468
75	0.5	1200	48.0	6.0	15.0	12.66	0.0468
75	0.1	1200	12.6	9.5	15.0	12.66	0.0468

behavior (or the shape of the calculated curves). Thus, if the oxidation is not carried out for a sufficient length of time, all models may approximately describe the experimental results, and one may erroneously conclude that a particular model is "correct." In this respect it may be noted that Pettit and B. Wagner only followed the oxidation to weight gains of about 32 mg/cm^2 (see Fig. 7).

2. For plots of $(\Delta m/A)^2$ vs. time, as shown in Figs. 7 and 8, the curves are according to the classical model expected to have a continuously increasing gradient toward a final value. In this respect the experimentally determined curves are basically different since typically, after some period of reaction, they show constant gradients as for parabolic oxidation.
3. As regards the calculated values for extended oxidation it is found that the best overall fit is obtained if it is assumed that the values of n change with the experimental conditions (i.e., the defect structure or mechanism of the surface reaction changes with gas pressure and time). By way of example, at 1000°C the best fit is for n between 1.5–2.0 at 1 and 0.5 atm. total pressure, while at 0.1 atm. n is lower than 3. The general tendency is that the best values of n decrease with temperature, p_{CO_2} , and the total gas pressure. As regards values of n equal to 2 or 3, an important question becomes: What type of defect structure do these values of n reflect? The authors are not able to advance reasonable models for such values of n . In this respect it may be recalled that Grabke¹⁹ and Riecke and Bohnkamp²⁸ reported values of $n \leq 1$ for equilibrated wüstite specimens.

Other modifications of the classical model could alternatively be considered. Thus, one may speculate if the values of \tilde{D} and \mathcal{K} gradually change with time of oxidation and if this may bring the calculated values in better accord with the measured values. However, the authors cannot find any reasonable interpretation of the results on this basis and provisionally conclude that the experimental results deviate significantly from that predicted by the classical model.

Metallographic and X-Ray Diffraction Analyses of the Scales

In further studies of the overall reaction behavior, the oxide scales were studied by optical metallography, scanning electron microscopy (SEM), and x-ray diffraction.

Metallographic Studies

Optical metallography and SEM studies of the scales revealed that only a single phase, wüstite, was formed as a reaction product. This is, of course,

expected for exposures to gas mixtures where only wüstite is thermodynamically stable. But wüstite was also the only reaction product observed as long as an iron core was present beneath the scale even for reactions in CO₂ and CO₂-rich mixtures of CO₂ + CO, in which the oxygen activities are several orders of magnitude higher than those of oxygen equilibrium of wüstite/magnetite mixtures. For parabolic reaction behavior, an outer layer of magnetite would be expected to be formed. Such a layer could not be detected. The absence of an outer magnetite layer has also been reported by Smeltzer² for oxidation of iron in CO₂ at about 1000°C.

X-Ray Diffraction Analysis

Magnetite was only observed by x-ray diffraction as an orientationally related precipitated phase within the wüstite phase in scales reacted at 1200°C in CO₂-rich gas mixtures. In these scales, also, a "stoichiometric" wüstite phase, with a high lattice parameter equal to about 4.330 Å, and with the same

Table III.

% (CO ₂)	P _{tot} (atm)	Temp. (°C)	Δm/A (mg/cm ²)	a _(Fe_{1-x}O) (Å)	a _(FeO) (Å)	Magnetite (yes/no)
pure CO ₂	1	1000	71.0	4.2920 (20)	No	No
pure CO ₂	0.5	1000	65.6	4.0340 (20)	No	No
pure CO ₂	0.1	1000	82.5	4.3080 (20)	No	No
pure CO ₂	1	1200	78.0	4.2903 (15)	4.3200 (20)	Yes
95	1	1200	65.0	4.2870 (10)	4.3330 (20)	Yes
95	0.5	1200	65.0	4.3020 (20)	No	No
90	1	1200	105.0	4.2930 (10)	4.3320 (10)	Yes
75	1	1200	162.7	4.2910 (10)	4.3310 (20)	Yes
75	1	1200	81.6	4.2925 (10)	No	No
75	0.5	1200	80.6	4.2950 (10)	No	No
75	0.1	1200	83.4	4.3040 (10)	No	No

orientation as the wüstite scale, was observed. This feature is illustrated in Table III, where column 4 shows the weight gain of the specimens at the time of the quench. From these results it is concluded that the observed magnetite is formed by decomposition of wüstite due to the instability of wüstite at temperatures below 570°C. The decomposition always resulted in "stoichiometric" wüstite and magnetite, without any traces of an iron phase. The results in Table III also suggest that magnetite and stoichiometric wüstite are formed in specimens quenched from 1200°C only when the lattice parameter is less than about 4.292 Å.

In an attempt to characterize the nonstoichiometry of the wüstite surface during oxidation, x-ray diffraction measurements directly on the surface of scales quenched during oxidation were performed. A basis for these studies is that the lattice parameter varies with the nonstoichiometry of wüstite.

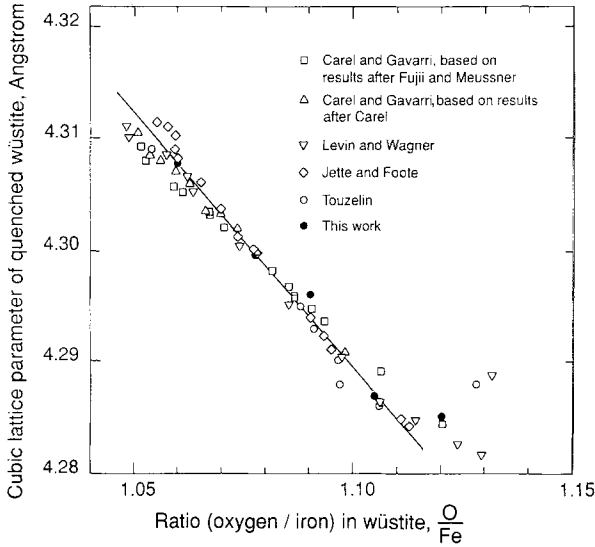


Fig. 9. The cubic lattice parameter in equilibrated and quenched wüstite as a function of the oxygen/iron ratio in wüstite. The graph also includes previously reported results by Carel and Gavarri,²⁹ Levin and Wagner,³⁰ Jette and Foote,³¹ and Touzelin.³²

This variation is illustrated in Fig. 9, which shows some literature values of quenched wüstite specimens after equilibration in various $\text{CO}_2 + \text{CO}$ mixtures.²⁹⁻³² In the composition region, $1.06 < \text{O}/\text{Fe} < 1.10$, the agreement between different investigations is satisfactory. As reference, corresponding measurements were made in this work, and as seen in Fig. 9 (the results are also listed in Table IV) our values of the lattice parameter are in accord with previously reported results.

The relation between the cubic lattice parameter, a , and the composition may (following these results) be expressed by

$$a = -0.4099 \frac{\text{O}}{\text{Fe}} + 4.7414 \quad (25)$$

When one combines this relation with that between oxygen activity and the O/Fe ratio [see Eqs. (10) and (11)], the following relations are obtained between the lattice parameter and the equilibrium oxygen activity of the ambient gas:

$$\log a_{\text{O}}^* = 11.664 \left(\frac{4.7414 - a}{0.4099} \right) - 12.626 \quad (1000^\circ\text{C}) \quad (26a)$$

and

$$\log a_{\delta}^* = 12.078 \left(\frac{4.7414 - a}{0.4099} \right) - 13.170 \quad (1200^{\circ}\text{C}) \quad (26b)$$

Measurements of the lattice parameter directly on the surface of quenched oxidized specimens may on this basis provide information on the oxygen activity within a surface layer of the scales.

Table IV shows the results of the lattice parameter determinations of wüstite on specimens reacted at 1000 and 1200°C in 75%CO₂+25%CO at different total gas pressures. In this table the measured values are also compared with values that may be estimated using the classical model [i.e., parameters have been estimated through Eqs. (26) from the calculated values of the oxygen activity in the surface (a_{δ}^*)]. In this connection it should be recalled that the calculated values of the oxygen activities depend on the function $f(a_{\delta}^*)$ (i.e., on the values of n in a_{δ}^{*-n}). Corresponding lattice parameters have been calculated for different values of n , and Table IV shows the values for $n=2/3$, 1.5, 2, and 3, respectively. The comparison between the measured and calculated values shows that the best agreement is obtained for values ranging from about 1.5 to 2.

The salient point of these results is that the oxygen activity (deviation from stoichiometry) in the surface layer is always lower than that expected for a value of $n=2/3$ as was deduced by Grabke from measurements on equilibrated wüstite specimens.

All in all, x-ray diffraction studies support the conclusion drawn from the rate measurements that the experimental results deviate significantly from that predicted by the classical model. Alternative interpretations are needed.

Alternative Models

There may be several reasons for the failure of the classical model to properly describe oxidation of iron in CO₂+CO mixtures at high temperatures.

An important assumption in the classical model is that the predominant defects and their concentrations at or close to the wüstite surface during oxidation are exactly the same as in the bulk material, and also equal to that in bulk wüstite equilibrated in the same atmospheres. Any effect due to slow equilibration and surface effects are neglected. It is not unreasonable to question such an assumption in view of the large number of studies of structures and compositions of surfaces that have been carried out over the

Table IV.

Sample characteristics		Calc. O ₂ activity/lattice parameter for $f(a\bar{c}) = (a\bar{c})^{-n}$												Meas. lattice parameter ^a (Å)			
% (CO ₂)	P _{tot} (atm)	T (°C)	Δm/A (mg/cm ²)	Oxygen activity, $(a\bar{c})^{-n}$			Lattice parameter, Å			n = 3	n = 2	n = 1.5	n = 2/3		n = 1.5	n = 2	n = 3
				n = 2/3	n = 1.5	n = 2	n = 3	n = 2/3	n = 1.5					n = 2			
75	1	1000	54.0	1.0360	0.8403	0.7786	0.7049	4.2971	4.3003	4.3015	4.3030	4.3030	4.3030	4.3030	4.3030	4.3030	4.3030 (10)
75	1	1000	82.0	1.2550	0.9617	0.8716	0.7669	4.2942	4.2983	4.2998	4.3017	4.3017	4.3017	4.3017	4.3017	4.3017	4.3000 (10)
75	0.1	1000	45.0	0.4602	0.4551	0.4534	0.4490	4.3095	4.3097	4.3098	4.3100	4.3100	4.3100	4.3100	4.3100	4.3100	4.3120 (10)
75	0.1	1000	57.0	0.4767	0.4697	0.4659	0.4604	4.3090	4.3092	4.3094	4.3095	4.3095	4.3095	4.3095	4.3095	4.3095	4.3130 (10)
75	0.1	1000	94.0	0.5256	0.5072	0.4994	0.4877	4.3075	4.3080	4.3082	4.3086	4.3086	4.3086	4.3086	4.3086	4.3086	4.3065 (10)
75	1	1200	34.5	1.2770	0.9652	0.8721	0.7645	4.2908	4.2950	4.2965	4.2984	4.2984	4.2984	4.2984	4.2984	4.2984	4.3005 (10)
75	1	1200	58.2	1.6151	1.1600	1.0200	0.8610	4.2874	4.2923	4.2941	4.2966	4.2966	4.2966	4.2966	4.2966	4.2966	4.2945 (10)
75	1	1200	81.6	1.8403	1.3030	1.1270	0.9303	4.2855	4.2905	4.2927	4.2955	4.2955	4.2955	4.2955	4.2955	4.2955	4.2925 (10)
75	1	1200	84.0	1.8596	1.3170	1.1380	0.9367	4.2853	4.2904	4.2925	4.2954	4.2954	4.2954	4.2954	4.2954	4.2954	4.2940 (10)
75	1	1200	162.7	2.2600	1.6692	1.3800	1.1226	4.2824	4.2869	4.2897	4.2927	4.2927	4.2927	4.2927	4.2927	4.2927	4.2910 (10)
75	0.5	1200	80.6	1.3868	1.0020	0.8906	0.7630	4.2896	4.2944	4.2961	4.2984	4.2984	4.2984	4.2984	4.2984	4.2984	4.2950 (10)
75	0.1	1200	53.4	0.5641	0.5104	0.4914	0.4663	4.3029	4.3044	4.3049	4.3057	4.3057	4.3057	4.3057	4.3057	4.3057	4.3080 (15)
75	0.1	1200	83.4	0.6796	0.5789	0.5464	0.5057	4.3001	4.3025	4.3033	4.3045	4.3045	4.3045	4.3045	4.3045	4.3045	4.3040 (10)
75	1	1200	Equil.														4.2853 (07)
64.7	1	1200	Equil.														4.2870 (05)
50	1	1225	Equil.														4.2996 (07)
50	1	1200	Equil.														4.2963 (07)
50	0.5	1200	Equil.														4.2967 (07)
30	1	1200	Equil.														4.3068 (07)

^aThe uncertainty in the last two figures is indicated by parentheses.

years with advanced instrumental techniques. These have clearly demonstrated significant differences between properties of surfaces and bulk material and have generally revealed important and significant enrichment and segregation phenomena at surfaces of components both from the ambient atmosphere and from the bulk.³³⁻⁴²

When iron is reacted in CO₂ and CO₂ + CO mixtures at high temperatures, the reaction product is wüstite. Following Grabke⁴³ the equilibrium carbon solubility in bulk wüstite is extremely low and on the order of but a few ppm. Accordingly, any overall carbon uptake should be insignificant relative to the overall weight gain during the reaction.

But still the question remains if carbon in some form interacts and becomes enriched in and near the surface. If so, it may be argued that this may significantly affect the defect structure and defect concentrations in or near the surface. This may, in turn, change the defect gradient of the diffusing defects through the scale and thereby affect the reaction rate compared to that in carbon-free environments.

In this respect it is important to summarize some of the main aspects of the experimental results: (i) The oxidation in CO₂ and CO₂ + CO mixtures (with total pressures equal to or less than atmospheric pressure) is slower than in oxygen. (ii) The parabolic oxidation and corresponding rate constants evaluated from our measurements are not only dependent on the oxygen activity of the ambient gas as assumed in the classical model, but also on the partial pressure of CO₂ and the total pressure of the CO₂ + CO mixture. (iii) The oxidation is slower and the nonstoichiometry of wüstite near the outer surface of the scale is smaller than that predicted by the classical model when assuming that the properties of equilibrated wüstite is equal to that of growing wüstite scales. (iv) As far as can be determined, wüstite is the only reaction product even in CO₂ and CO₂-rich CO₂ + CO mixtures with oxygen activities several orders of magnitude higher than that needed for formation of magnetite. An additional aspect is that the parabolic rate constant in H₂O + H₂ mixtures are higher than in CO₂ + CO mixtures with the same oxygen activity. These results suggest that one or more additional factors must be taken into account in interpreting the reaction mechanism.

Another important aspect is the question of the nature of the defect structure and the diffusing species in growing wüstite scales as compared to that in equilibrated wüstite. Structural studies on equilibrated (and usually quenched) specimens of wüstite have shown that the defects predominantly consist of defect clusters containing iron vacancies and interstitials in ratios ranging from 3:1 to 4:1. In analogy with formation of extended defects in high temperature oxides in general, it would not be unexpected that the formation of defect clusters with varying degree of complexity would be

slow and that extended time periods would be needed to obtain true defect equilibria.⁴⁴ In this respect it is, for instance, interesting to examine published results on the self-diffusion of iron in wüstite. These show significant discrepancies; importantly, the self-diffusion of iron has been reported to increase and decrease with increasing deviation from stoichiometry in the temperature range 800–1000°C.^{10,45–48}

In growing wüstite scales the defects, and particularly the complexity of the defect clusters, may in these terms be expected to be different from that of wüstite, which has been equilibrated for extended time periods. Furthermore, in growing scales, new defects are being continuously formed at the outer scale surface and migrate inward through the scale.

At this time it is not possible to determine the exact nature of the migrating defects in growing scales. But as a general conclusion, it would not be unexpected that the defects and defect structures in growing scales may differ in complexity from those in equilibrated wüstite. From this it follows that defect-dependent properties as measured on equilibrated wüstite (e.g., self-diffusion of iron) may not necessarily be applied in transport equations, as for instance in the classical Wagnerian theory for parabolic oxidation.

In this connection the question of nonstoichiometry in growing wüstite scales may also be raised. In wüstite equilibrated in CO₂ + CO mixtures the composition is approximately Fe_{0.95}O at the lower end of the wüstite field (i.e., at the iron/wüstite boundary). This large deviation from stoichiometry may—at least partially—be related to the stabilizing effect of defect clusters. If the concentration of mobile defect clusters or iron vacancies are smaller in growing scales than in equilibrated wüstite, the question arises if the deviation from stoichiometry at the iron/wüstite boundary of growing scales is smaller than in equilibrated wüstite. Such an effect should in case be reflected in the parabolic rate constant for growth of wüstite scales.

Due to these many unanswered questions, it does not appear possible to give an unequivocal interpretation of the reaction mechanism of growth of wüstite scales. But even so—and particularly on the basis of the observed gas pressure dependencies—it is of interest to suggest limiting models for the reaction mechanisms.

Linear Oxidation

As shown above, the gas pressure dependence of the linear oxidation rate constant as evaluated from the general linear/parabolic equation may, at both 1000 and 1200°C, be expressed as

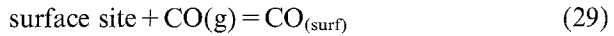
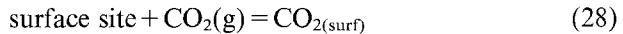
$$k_{\text{lin}} = k_{\text{lin}}^0 N_{\text{CO}_2} p_{\text{CO}_2} \quad (27)$$

where k_{lin}^0 is a constant.

The same gas pressure dependence also applies to the maximum rates of the reaction, k_{\max} .¹⁰ The values of k_{lin} are, however, somewhat larger than the values of k_{\max} . This is concluded to reflect that the reorientation of the initial scales is incomplete at the maximum rates of reaction, while k_{lin} , which is determined from later stages of the reaction, represents the linear reaction for reoriented scales.

With regard to k_{lin} , it may be noted that the linear/parabolic equation [Eq. (19)] implies that the concentration of diffusing species at the oxide/gas interface is constant with time. This is in contrast to the classical model, where the concentration of the migrating defects at the scale/gas interface is assumed to increase gradually toward the final equilibrium value.

The fact that k_{lin} is dependent on the mole fraction of CO₂ (and thus the total gas pressure) indicates that the reaction mechanism of the surface reaction depends on the partial pressures of both CO₂ and CO in the ambient atmosphere. A possible interpretation of the observed gas pressure dependence is that both CO₂ and CO interacts with the wüstite surface to form corresponding surface complexes (or adsorbed species) and that the rate-determining reaction with CO₂ + CO preferentially takes place at the sites of the CO₂-surface complexes. The formation of the surface complexes may be written



where CO_{2(surf)} and CO_(surf) represent the surface complexes of the two gases.

The total number of surface complexes [assuming for simplicity only those given in Eqs. (28) and (29)] is then given by

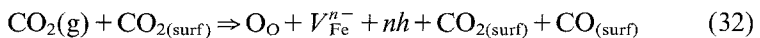
$$\text{CO}_{2(\text{surf})} + \text{CO}_{(\text{surf})} = k_1 p_{\text{CO}_2} + k_2 p_{\text{CO}} \quad (30)$$

where k_1 and k_2 are equilibrium constants. The fraction of CO₂-surface complexes, Θ_{CO_2} is further given by

$$\Theta_{\text{CO}_2} = \frac{k_1 p_{\text{CO}_2}}{k_1 p_{\text{CO}_2} + k_2 p_{\text{CO}}} \quad (31)$$

If k_1 is approximately equal to k_2 , the fraction of CO₂-surface complexes is then given by N_{CO_2} .

Let us assume that the number of surface complexes are constant with time and that the CO₂ molecules react preferentially at the CO₂-surface complexes. The rate of formation of oxide may then be written



If this is the rate-determining reaction, the overall linear reaction may then be expressed by

$$k_{\text{lin}} = k_{\text{lin}}^0 N_{\text{CO}_2} p_{\text{CO}_2} \quad (33)$$

where k_{lin}^0 is the rate constant of the part reaction.

This is the observed gas pressure dependence. It is emphasized that this is only advanced as a possible model and that other alternative models may be considered.

Parabolic Oxidation

Diffusion-controlled parabolic growth of scales implies that the concentration of the diffusing species at the interfaces of the scale is nearly constant with time. For wüstite, which is metal-deficient, the migrating defect or defects are continually being formed at the wüstite/gas interface, and it is the defect concentration at this interface that primarily accounts for the gas pressure dependence of the parabolic rate constant.

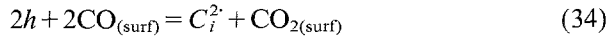
In the classical model, it is assumed that the defect concentration at the scale/gas interface is only determined by the oxygen activity. This is determined by the ratio of p_{CO_2} to p_{CO} [i.e., $a_{\text{O}} = K(p_{\text{CO}_2}/p_{\text{CO}})$, where K is the equilibrium constant]. Accordingly, the reaction rate and parabolic rate constant should only be dependent on the ratios of the partial pressures of CO_2 and CO , and not on the total pressure of the gas mixture. This is not in accord with the experimental results as for instance illustrated in Fig. 5. These results indicate that at least one more factor also has to be considered in the reaction mechanism. As carbon is the only other component beside iron and oxygen in the overall system, it is reasonable to ask if carbon may influence the reaction behavior. As carbon only dissolves in minute amounts in single crystals of wüstite equilibrated in $\text{CO}_2 + \text{CO}$ mixtures, it should not affect the defect concentrations in the wüstite lattice as a dopant. Any major effect of carbon on the scale growth of wüstite scales would thus be expected to be at the interfaces of the scale, and particularly at the scale/gas interface. Let us consider this possibility.

How and in what form can carbon affect or determine the concentrations of migrating iron defects at the wüstite/gas interface? As the detailed diffusion mechanism and the nature of migrating iron defects (e.g., single vacancies, defect clusters, or migration of single vacancies from one cluster to another) is not known, it does not appear possible at this stage to make any unequivocal interpretation of the reaction mechanism and to describe in detail the defect structure situation at or near the surface. But let us assume that carbon can dissolve in some form in an extremely thin surface layer of the wüstite scale. Such an assumption is not unreasonable in view of the results of Freund *et al.*,³³⁻³⁷ who have shown in extensive studies on

MgO that carbon becomes enriched in a surface layer with a thickness of a few tens of Angstrom. An enrichment of carbon in the wüstite surface has also been indicated in the present study through scanning Auger microscopy (SAM),⁴⁹ but as carbon is an ever-present impurity under numerous conditions their latter results cannot be taken as a definite proof of the presence of carbon under the reaction conditions.

Let us assume for the sake of illustration that carbon dissolves as interstitial ions in a thin surface layer due to a stabilizing effect on the surface energy. The carbon ions are probably not present as a single, unassociated ion, but are rather associated with an oxygen ion on a normal oxygen site.³⁷ However, in terms of defect equations and electroneutrality conditions, these alternative models are equivalent; and for the sake of clarity, the interstitial carbon ions are described in the following as C_i species rather than as associated species with oxygen (e.g., CO_O). The very same differences in notation of defects applies to interstitial hydrogen ions/defects in metal oxides.⁵⁰

As an illustration of a limiting model, let us assume that the interstitially dissolved carbon ions in the surface layer during parabolic oxidation are formed through, and are in equilibrium with, the CO₂-surface complexes:

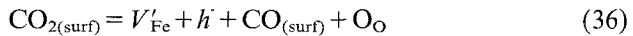


which gives the equilibrium

$$p^2[\text{CO}_{(\text{surf})}]^2 = K_{35}[C_i^{2'}][\text{CO}_{2(\text{surf})}] \quad (35)$$

where K_{35} is the equilibrium constant.

Let us further assume that oxygen is incorporated and iron vacancies formed in the surface layer through the equilibrium with CO₂-surface complexes. If for the sake of illustration the vacancies are assumed to have one negative effective charge, this equilibrium may be written



The corresponding defect equilibrium is given by

$$[V'_{\text{Fe}}]p = \frac{K_{37}[\text{CO}_{2(\text{surf})}]}{[\text{CO}_{(\text{surf})}]} \quad (37)$$

Let it finally be assumed that the electroneutrality condition in the surface layer is

$$2[C_i^{2'}] = [V'_{\text{Fe}}] \quad (38)$$

By combining Eqs. (35), (36), and (38), it is seen that the concentration of iron vacancies is given by

$$[V'_{\text{Fe}}]^3 = K_{39}[\text{CO}_2(\text{surf})] \quad (39)$$

where K_{39} is equal to $2K_{37}^2/K_{35}$.

Let it be assumed that the mass transport takes place via so-called (4:1) clusters consisting of four iron vacancies and one interstitial iron. The formation of (4:1) clusters may be written



and the corresponding defect equilibrium is given by

$$[V'_{\text{Fe}}]^3 = K_{41}[(4:1)''''] \quad (41)$$

where K_{41} is a constant. Combining Eqs. (41) and (39) gives

$$[(4:1)''''] = K_{42}[\text{CO}_2(\text{surf})] \quad (42)$$

where $K_{42} = 2K_{37}^2/K_{35}K_{41}$. Finally, assuming that the fraction of CO_2 surface complexes is equal to N_{CO_2} and that the mole fraction of CO_2 describes the activity of these species on the surface [see Eq. (31)], the concentration of mobile defects is given by

$$[(4:1)''''] = K_{43}N_{\text{CO}_2} \quad (43)$$

where K_{43} is a constant.

The parabolic rate constant may be expressed under simplified conditions by

$$k_p = K_{44} \cdot \{[(4:1)''''] - [(4:1)''''_{(\text{Fe}/\text{Fe}_{1-x}\text{O})}]\} \quad (44)$$

where K_{44} is constant and $[(4:1)''''_{(\text{Fe}/\text{Fe}_{1-x}\text{O})}]$ is the defect concentration at the metal/scale interface, and $[(4:1)'''']$ at the outer surface. Thus, if the concentration of mobile defects at the inner interface is much lower than at the outer interface, then k_p may according to this model be written

$$k_p = K_{44}N_{\text{CO}_2} \quad (45)$$

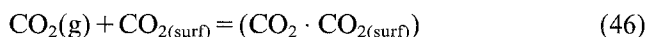
The experimentally measured parabolic rate constant in $\text{CO}_2 + \text{CO}$ mixtures at 1200°C may be expressed as, following Fig. 6,

$$k_p = K_{41} \cdot N_{\text{CO}_2} p_{\text{CO}_2}^{0.1}$$

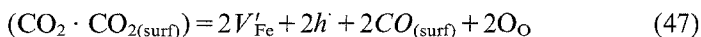
This is approximately the same as for the model considerations. A few comments should be made about the expressions in Eqs. (21) and (22) for the measured values of k_p . If N_{CO_2} becomes lower than the value necessary to stabilize wüstite with respect to iron, oxidation will not take place. Thus, a critical number of surface complexes exist for oxidation to take place.

Furthermore, as the partial pressure of CO₂ becomes very low, k_p approaches zero. So, if the number of mobile defects depends on p_{CO_2} , this may indicate that the concentration of mobile defects at the iron/wüstite interface is relatively small, and this may in turn, indicate that the total deviation from stoichiometry at this interface is small. If this interpretation is correct, it indicates that the defect structure situation in growing layers is different from equilibrated wüstite (which has a significant deviation from stoichiometry at this interface).

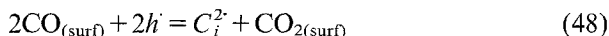
At this stage we are not able to advance a consistent expression for k_p including both a dependence of the partial pressure of CO₂ and the mole ratio of CO₂ in the gas mixture. However, just to indicate how an expression for [(4:1)^m], which depend on p_{CO_2} may be derived, assume that CO₂ may interact with CO_{2(surf)} [see also Eq. (32)].



where (CO₂ · CO_{2(surf)}) is a surface complex. These complexes may produce iron defects through the defect reaction



Furthermore, we also have



In a similar procedure as above, and using the electroneutrality condition given by Eq. (38), the following expression may be derived

$$[V'_{\text{Fe}}]^3 = K_{49} p_{\text{CO}_2} \quad (49)$$

which gives

$$[(4:1)^m] = K_{50} p_{\text{CO}_2} \quad (50)$$

where K_{49} and K_{50} are constants.

Numerous other modifications or variations of the same type of models and mechanisms may be advanced. One may alternatively consider that the defects have different effective charges; that coulombic interactions also take place between the positively charged interstitial carbon and the negatively charged iron vacancies; that iron defect clusters, with or without carbon, are formed, etc. However, further modeling at this stage is postponed until more detailed results and information on the defect structure situation in surfaces of this system have become available.

A comment should also be made regarding the absence of a thin outer layer of magnetite under ambient conditions when bulk thermodynamic (equilibrium) properties of wüstite and magnetite predict that magnetite should be formed. No unequivocal interpretation can be given, but it is

interesting to speculate if this is related to the smaller deviations from stoichiometry in the outer layer of the wüstite scales when exposed to CO_2 and $\text{CO}_2 + \text{CO}$ mixtures, and that the defect concentration in growing scales is different from that of equilibrated wüstite specimens.

SUMMARY AND CONCLUDING REMARKS

In this work, high purity iron has been oxidized in CO_2 and $\text{CO}_2 + \text{CO}$ mixtures with various total gas pressures ranging from 0.1 to 1 atm. The studies have included measurements of the reaction kinetics, and characterization of the resulting wüstite scales by means of metallography, scanning electron microscopy, and x-ray diffraction.

The oxidation comprises coupled linear/parabolic kinetics. The results have been analyzed in terms of a classical model for which a basic assumption is that the surface of the wüstite scales have exactly the same composition and defect structure as that of the bulk and that of wüstite equilibrated in the same atmospheres. This model implies that the defect concentration (nonstoichiometry) in the wüstite surface gradually increases with time until a final equilibrium value is reached after extended reaction and when true parabolic kinetics are followed. This model predicts that under limiting conditions:

1. The linear rate is proportional to the partial pressure of CO_2 .
2. The parabolic rate constant is only dependent on the oxygen activity of the ambient gas under conditions when only wüstite may be formed and independent of the ambient oxygen activity under conditions when a thin surface layer of magnetite is expected to be formed. The parabolic rate constant is furthermore, expected to be the same in oxygen, and in CO_2 -rich mixtures of $\text{CO}_2 + \text{CO}$.

The experimental results are not in accord with these predictions:

1. Both the linear and parabolic rate constant are found to be dependent both on the composition and the total gas pressure of the ambient $\text{CO}_2 + \text{CO}$ mixtures. Both rate constants decrease with decreasing total gas pressure.
2. The parabolic rate constants are smaller in CO_2 and $\text{CO}_2 + \text{CO}$ mixtures (at and below 1 atm. total gas pressure) than in oxygen gas. The parabolic rate constant in $\text{CO}_2 + \text{CO}$ mixtures is also smaller than in $\text{H}_2\text{O} + \text{H}_2$ mixtures with the same oxygen activities.
3. Wüstite is the only reaction product at 1000–1200°C as long as an unoxidized iron core is present beneath the wüstite scale. It has not been possible to detect magnetite as a thin outer layer under conditions when the ambient gas atmospheres have oxygen activities which

are orders of magnitude higher than that needed to oxidize wüstite to magnetite.

4. The lattice parameter in an outer layer of the wüstite scales is larger and thus the iron deficit is smaller than that predicted from the classical model.

Unequivocal interpretations cannot as yet be made of the real reaction mechanisms, but the following aspects are proposed to be important:

1. Both CO and CO₂ molecules interact with the wüstite surface to form surface complexes, and the surface reaction involves a preferential incorporation of oxygen from adsorbed CO₂ molecules at the CO₂-surface complexes.
2. The defect structure in the wüstite surface exposed to CO₂ and CO₂ + CO mixtures is different from that of wüstite surfaces exposed to oxygen gas only, and specifically it is suggested that carbon ions interstitially dissolved in a thin surface layer, in turn, affects the defect gradient through the scale and thereby the parabolic rate constant.
3. The question is simultaneously raised if the defect structure and diffusing species in growing wüstite scales are different from those in wüstite equilibrated for extended periods in the same gas mixtures.

It is interesting to speculate if the same type of phenomena are important for other systems. For instance, are similar effects important for corrosion of metals in oxygen-sulfur containing atmospheres, sulfidation of metals in S₂ and H₂ + H₂S mixtures, etc. In this respect it is interesting to note that for corrosion in oxygen-sulfur-containing gases, transitions from sulfide to oxide formation seldom takes place at the values predicted from bulk thermodynamic properties of the corresponding sulfides and oxides.²¹

ACKNOWLEDGMENT

The authors wish to express sincere thanks to Professor Nico Norman, who carried out the x-ray diffraction analysis, for the valuable discussions during the course of this work.

REFERENCES

1. K. Hauffe and H. Pfeiffer, *Z. Metallk.* **44**, 27 (1953).
2. W. W. Smeltzer, *Acta Met.* **8**, 377 (1960).
3. F. S. Pettit, R. Yinger, and J. B. Wagner, Jr., *Acta Met.* **8**, 617 (1960).
4. F. S. Pettit and J. B. Wagner, Jr., *Acta Met.* **12**, 35 (1964).
5. K. Hedden and G. Lehmann, *Arch. Eisenhüttenwesen* **35**, 839 (1964).
6. L. A. Morris and W. W. Smeltzer, *Acta Met.* **15**, 1591 (1967).

7. E. T. Turkdogan and J. V. Vinters, *Met. Trans.* **3**, 1561 (1972).
8. S. M. El Rahgy, F. Jeannot, and C. Gleitzer, *J. Mater. Sci. Lett.* **13**, 2510 (1978).
9. R. Bredesen and Per Kofstad, *Oxid. Met.* **34**, 361 (1990).
10. R. Bredesen and Per Kofstad, *Oxid. Met.* **35**, 107 (1991).
11. W. W. Smeltzer, *Trans. Met. Soc. AIME* **218**, 674 (1960).
12. C. Wagner, *Ber. Bunsenges.* **70**, 775 (1966).
13. L. S. Darken and R. W. Gurry, *J. Am. Ceram. Soc.* **67**, 1398 (1945).
14. P. Vallet and P. Raccach, *Mem. Sci. Rev. Met.* **62**, 1 (1965).
15. R. J. Ackermann and R. W. Sandford, Tech. Rept. ANL-7250 (September 1966), p. 46.
16. B. Swaroop and J. B. Wagner, Jr., *Trans. AIME* **239**, 1215 (1967).
17. H. G. Sockel and H. Schmalzried, *Ber. Bunsenges. Phys. Chem.* **72**, 745 (1968).
18. R. A. Giddings and R. S. Gordon, *J. Am. Ceram. Soc.* **56**, 111 (1973).
19. H.-J. Grabke, *Ber. Bunsenges. Phys. Chem.* **69**, 48 (1965).
20. B. Pieraggi, *Oxid. Met.* **27**, 177 (1987).
21. P. Kofstad, in *High Temperature Corrosion* (Elsevier, New York, 1988).
22. E. T. Turkdogan, W. M. McKewan, and L. Zwell, *J. Phys. Chem.* **69**, 327 (1965).
23. F. Nardou, P. Raynaud, and M. Billy, *J. Chim. Phys.* **76**, 595 (1979).
24. R. L. Levin and J. B. Wagner, Jr., *Trans. Met. Soc. AIME* **233**, 159 (1965).
25. L. W. Laub and J. B. Wagner, Jr., *Oxid. Met.* **7**, 1 (1973).
26. F. Millot and J. Berthon, *J. Phys. Chem. Solids* **47**, 1 (1986).
27. A. Sadowski, G. Petot-Ervas, C. Petot, and J. Janowski, *Proc. of the Third Round Table Meeting on Physico-Chemical and Structural Properties and Kinetics of Reduction of Wüstite and Magnetite* (Sept. 28–Oct. 3 1986, Jadwisin, Poland), in *Metallurgia I Odlewnictwo*, p. 259.
28. E. Riecke and K. Bohnenkamp, *Arch. Eisenhüttenw.* **40**, 717 (1969).
29. C. Carel and J. R. Gavarri, *Mater. Res. Bull.* **11**, 745 (1976).
30. R. L. Levin and J. B. Wagner, Jr., *Trans. Met. Soc. AIME* **236**, 516 (1966).
31. E. R. Jette and F. Foote, *J. Chem. Phys.* **1**, 29 (1933); *AIME Trans.* **105**, 276 (1933).
32. B. Touzelin, *Proc. of the Third Round Table Meeting on Physico-Chemical and Structural Properties and Kinetics of Reduction of Wüstite and Magnetite* (Sept. 28–Oct. 3 1986), Jadwisin, Poland, in *Metallurgia I Odlewnictwo*, p. 107.
33. F. Freund, G. Debras, and G. Demortier, *J. Am. Ceram. Soc.* **61**, 429 (1978).
34. H. Wengler, R. Knobel, H. Katherin, G. Demortier, G. Wolff, and F. Freund, *J. Phys. Chem. Solids* **43**, 59 (1982).
35. H. Katherin and F. Freund, *J. Phys. Chem. Solids* **44**, 177 (1983).
36. H. Katherin, H. Gonska, and F. Freund, *J. Appl. Phys.* **A30**, 33 (1983).
37. F. Freund, *Proc. of "Science of Ceramics 13"* (Orléans, France, 1985), publ. in *The Journal de Physique* 1986, P. Odier, F. Cabannes, and B. Cales, eds., p. 499.
38. J. Nowotny, *Mater. Sci. Forum* **29**, 99 (1988).
39. J. Nowotny, in *Surfaces and Interfaces of Ceramic Materials* (1989), p. 205.
40. R. G. Egdell and W. C. Mackrodt, in *Surfaces and Interfaces of Ceramic Materials* (1989), p. 185.
41. J. M. Blakely and S. M. Mukhopadhyay, in *Surfaces and Interfaces of Ceramic Materials* (1989), p. 285.
42. R. G. Egdell and W. C. Mackrodt, *J. Am. Ceram. Soc.* **72**, 1576 (1989).
43. I. Wolf and H.-J. Grabke, *Solid State Commun.* **54**, 5 (1985).
44. R. S. Roth, *Solid State Chem.* **13**, 159 (1980).
45. L. Himmel, R. F. Mehl, and C. E. Birchenall, *Trans. AIME* **197**, 827 (1953).
46. P. Desmaescaux, J. P. Boquet, and P. Lacombe, *Bull. Soc. Chim. Fr.* **15**, 1106 (1965).
47. P. Hembree and J. B. Wagner, Jr., *Trans. Met. Soc. AIME* **245**, 1547 (1969).
48. W. K. Chen and N. L. Peterson, *J. Phys. Chem. Solids* **36**, 1097 (1975).
49. R. Bredesen and P. Kofstad, *Proc. of The Third Round Table Meeting on Physico-Chemical and Structural Properties and Kinetics of Reduction of Wüstite and Magnetite* (Sept. 28–Oct. 3 1986), Jadwisin, Poland, in *Metallurgia I Odlewnictwo*, p. 225.
50. T. Norby, in *Selected Topics in High Temperature Chemistry*, Ø. Johannesen and A. Andersen, eds. (Elsevier, Amsterdam, 1989), p. 101.